



UNIVERSITI PUTRA MALAYSIA

**EFFECTS OF SEGMENTATION AND STEP SAMPLING
ON APODIZED FIBER BRAGG GRATING**

MOHAMMAD M. N. AHMAD

FK 2002 29

**EFFECTS OF SEGMENTATION AND STEP SAMPLING ON APODIZED
FIBER BRAGG GRATING**

By

MOHAMMAD M. N. AHMAD

**Thesis Submitted to the School of Graduate Studies, Universiti Putra Malaysia, in
Fulfillment of the Requirements for the Degree of Master of Science**

September 2002



DEDICATION

To The Martyrs of Palestine

Abstract of thesis presented to the Senate of Universiti Putra Malaysia is fulfillment of the requirement for the degree of Master of Science

EFFECTS OF SEGMENTATION AND STEP SAMPLING ON APODIZED FIBER BRAGG GRATING

By

MOHAMMAD M. N. AHMAD

September 2002

Chairman : Associate Professor Mohamad Khazani Abdullah, Ph.D.

Faculty : Engineering

Practical implementation of apodized fiber Bragg grating results in approximation to the apodization profile. In this study, these profiles are simulated by sampling and segmentation. Segmenting an ideal profile is basically producing its corresponding piecewise linear profile. The number of segments varies with the error value, which is defined as the maximum absolute difference between the segmented profile and the ideal one. The relationship between the error and the number of segments is found to be one to many. To study the process normal and DWDM gratings have been considered. The quality of the fiber Bragg gratings was investigated through the maximum reflectivity, the SLSR, and the bandwidth of the normal gratings, the insertion loss, the bandwidth, and the crosstalk parameters for the DWDM gratings.

Some of the results are unexpected. Segmentation enhances the quality of the gratings for some error values. For example, side lobe suppression ratio for normal grating apodized with segmented profile is improved by around 5.8dB at error of 0.015 compared to the grating apodized with smooth function. An enhancement of 0.5% on the

maximum reflectivity is also achieved for these normal gratings. For DWDM gratings the insertion loss is decreased by an amount of 0.002dB and the adjacent crosstalk is improved by an amount of around 2.5dB for some approximated Cosine apodization profile.

The study was also done to investigate the sampling effect. Sampling rate was varied for a fixed value of the maximum error. The study showed a good grating quality over a wide range of sampling. This would have an impact of relaxing the practical implementation of such process. In order to explain the results obtained, a criteria was formulated. This is based on the integration of error function. This criterion was instrumental in explaining the results.

Abstrak tesis yang dikemukakan kepada Senat Universiti Putra Malaysia sebagai memenuhi keperluan untuk ijazah Master Sains

**EFFECTS OF SEGMENTATION AND STEP SAMPLING ON APODIZED
FIBER BRAGG GRATING**

Oleh

MOHAMMAD M. N. AHMAD

September 2002

Pengerusi : Profesor Madya Mohamad Khazani Abdullah, Ph.D.

Faculti : Kejuruteraan

Pelaksanaan praktik bagi “apodized fiber Bragg grating” mengakibatkan penganggaran pada profil “apodization”. Dalam kajian ini, kami menganggarkan profil-profil ini dalam pensegmenan. Pembahagian untuk profil ideal asasnya adalah mengeluarkan sempadan profil “piecewise linear”. Bilangan bahagian-bahagian adalah berbeza dengan ralat kadar, yang mana telah di jelaskan sebagai perbezaan mutlak yang maksimum diantara profil yang dibahagikan dan profil ideal. Perhubungan antara ralat dan bilangan segmen telah banyak berlaku. Untuk mengkaji proses tersebut kami telah mengambil kira grating normal dan DWDM. Kualiti bagi “fiber Bragg gratings” telah dikaji melalui pemantulan maksimum, “SLSR”, dan “bandwidth” pada grating normal, “insertion loss”, “bandwidth” dan parameter “crosstalk” untuk grating DWDM.

Keputusannya tidak dapat diduga. Pembahagian telah mempertingkatkan kualiti bagi grating-grating untuk beberapa kadar ralat. Sebagai contoh, nisbah “side lobe suppression” untuk grating normal “apodized” dengan profil “segmented” telah di

tingkatkan lebih kurang 5.8dB pada ralat 0.015 berbanding dengan grating apodized dengan fungsi lancar. Satu peningkatan pada 0.05% ke atas pemantulan maksimum juga telah tercapai untuk grating-grating normal ini. Bagi grating DWDM “insertion loss”nya telah dikurangkan lebih kurang 0.002dB dan “adjacent crosstalk” telah ditingkatkan pada kadar 2.5dB.

Kajian telah dijalankan untuk mengkaji kesan “sampling”. Kadar “sampling” adalah berbeza pada kadar tetap untuk ralat maksimum. Kajian ini menunjukkan kualiti tetap ke atas pelbagai jenis “sampling”. Ini akan mengendurkan kesan proses perlaksanaan. Untuk menerangkan keputusan yang telah dicapai, satu kriteria telah di formulakan. Ini adalah berdasarkan kepada persepaduan fungsi ralat. Kriteria ini telah menjadi faktor dalam menerangkan rumusan kajian.

ACKNOWLEDGEMENTS

I express my appreciation and deep gratitude to Assoc. Prof. Dr. Mohamad Khazani Abdullah, for his wise council, guidance and encouragement that made this work possible. Grateful appreciation is extended to Dr. Ahmed Mohamed Almanasreh, for his worth ideas and guidance. Both have gone through each chapter of this research carefully to bring out an excellent quality of work. I would like also to extend my thanks to Assoc. Prof. Dr. Kaharudin Dimyati and Prof. Dr. Sahbudin Shaari for serving as my Supervisory Committee and providing precious suggestions and comments throughout my study.

Special thanks are expressed to all staff in Photronix (M) Sdn Bhd and for staff in the Photonic Laboratory of UPM who has contributed to the successful completion of this study. Grateful thanks are extended to Ragheb and Gulisthan Khalaf for their support and encouragement.

In the last, I would like to express my indebtedness to my mother, sisters, and brothers for their encouragements. I didn't forget my father who have been encouraging and supporting me to get higher educational degrees.

I certify that an Examination Committee met on 23rd September 2002 to conduct the final examination of Mohammad M. N. Ahmad on his Master of Science thesis entitled “Effects of Segmentation and Step Sampling on Apodized Fiber Bragg Gratings” in accordance with Universiti Pertanian Malaysia (Higher Degree) Act 1980 and Universiti Pertanian Malaysia (Higher Degree) Regulations 1981. The Committee recommends that the candidate be awarded the relevant degree. Members of the Examination Committee for the candidate are as follows:

Samsul Bahari Bin Mohd Nor, Ph.D.,
Lecturer,
Faculty of Engineering,
Universiti Putra Malaysia.
(Chairman)

Mohamad Khazani Abdullah, Ph.D.,
Associate Professor,
Faculty of Engineering,
Universiti Putra Malaysia.
(Member)

Kaharudin Dimyati, Ph.D.,
Associate Professor,
Faculty of Engineering,
Universiti Malaya.
(Member)

Sahbudin Shaari, Ph.D.,
Professor,
Faculty of Engineering,
Universiti Kebangsaan Malaysia.
(Member)

Ahmed Mohammed Almanasreh, Ph.D.,
Research & Development Manager,
Photronix (Malaysia) Sdn. Bhd.
(Member)



AINI IDERIS, Ph.D.,
Professor/Dean,
School of Graduate Studies,
Universiti Putra Malaysia.

Date: 23 OCT 2002

This thesis submitted to the Senate of Universiti Putra Malaysia has been accepted as fulfillment of the requirement for the degree of Master Science. The members of the supervisory Committee are as follows:

Samsul Bahari Bin Mohd Nor, Ph.D.,
Lecturer,
Faculty of Engineering,
Universiti Putra Malaysia.
(Chairman)

Mohamad Khazani Abdullah, Ph.D.,
Associate Professor,
Faculty of Engineering,
Universiti Putra Malaysia.
(Member)

Kaharudin Dimyati, Ph.D.,
Associate Professor,
Faculty of Engineering,
Universiti Malaya.
(Member)

Sahbudin Shaari, Ph.D.,
Professor,
Faculty of Engineering,
Universiti Kebangsaan Malaysia.
(Member)

Ahmed Mohammed Almanasreh, Ph.D.,
Research & Development Manager,
Photronix (Malaysia) Sdn. Bhd.
(Member)




AINI IDERIS, Ph.D.,
Professor/Dean,
School of Graduate Studies,
Universiti Putra Malaysia.

Date: 9 JAN 2003

DECLARATION

I hereby declare that the thesis is based on my original work except for quotations and citations, which have been duly acknowledged. I also declare that it has not been previously or concurrently submitted for any degree at UPM or other institutions.



MOHAMMADD M. N. AHMAD

Date: 23 Oct. 2002

TABLE OF CONTENTS

| | Page |
|-----------------------------|------|
| DEDICATION | ii |
| ABSTRACT | iii |
| ABSTRAK | v |
| ACKNOWLEDGEMENTS | vii |
| DECLARATION | x |
| LIST OF TABLES | xiii |
| LIST OF FIGURES | xiv |
| LIST OF ABBREVIATIONS | xvii |

CHAPTER

| | | |
|---|--|----|
| 1 | INTRODUCTION | 1 |
| | 1.1 Historical Prospective of FBG | 2 |
| | 1.2 Fiber Bragg Grating Applications in Telecommunications | 7 |
| | 1.3 Fiber Bragg Grating Applications in Sensing Systems | 8 |
| | 1.4 Problem Statement | 9 |
| | 1.5 Objectives | 11 |
| | 1.6 Methodology | 12 |
| | 1.7 Overview of Chapters | 14 |
| 2 | FIBER BRAGG GRATINGS | 15 |
| | 2.1 Introduction | 15 |
| | 2.2 Photosensitivity | 16 |
| | 2.3 FBG Properties | 17 |
| | 2.4 Types of Fiber Bragg Grating | 20 |
| | 2.4.1 Common Bragg Reflector | 20 |
| | 2.4.2 Blazed Bragg Grating | 21 |
| | 2.4.3 Chirped Gratings | 22 |
| | 2.4.4 Novel Bragg Grating Designs | 23 |
| | 2.5 Fiber Bragg grating Fabrication Techniques | 24 |
| | 2.5.1 Holographic Fabrication Techniques | 24 |
| | 2.5.1.1 Bulk (Amplitude Splitting) Interferometer | 25 |
| | 2.5.1.2 Wave Front Splitting Interferometers | 26 |
| | 2.5.1.3 Phase Mask Technique | 28 |
| | 2.5.2 Non-Holographic Techniques | 30 |
| | 2.5.2.1 Point-by-Point Fabrication Technique | 30 |
| | 2.5.2.2 Mask Image Projection | 31 |
| | 2.6 Fiber Bragg Grating Analysis | 32 |

| | | |
|-------|---|-----|
| 2.6.1 | Coupled Mode Theory | 34 |
| 2.6.2 | Fiber Bragg Grating | 35 |
| 2.6.3 | Transfer Matrix Method..... | 40 |
| 3 | LITERATURE REVIEW FOR APODIZING FIBER BRAGG GRATING . | 42 |
| 3.1 | Introduction | 42 |
| 3.2 | Apodization Profiles | 43 |
| 3.3 | Apodized Grating Fabrication Techniques | 47 |
| 3.3.1 | Self Apodization | 48 |
| 3.3.2 | Amplitude Mask Techniques | 50 |
| 3.3.3 | Variable Diffraction Efficiency Phase Mask | 51 |
| 3.3.4 | Multiple Printing of in Fiber Grating (MPF) | 52 |
| 3.3.5 | Moving Fiber/Phase Mask Technique | 52 |
| 3.3.6 | Symmetric Stretch Apodization Method | 54 |
| 3.4 | Conclusion | 55 |
| 4 | METHODOLOGY | 56 |
| 4.1 | Introduction..... | 56 |
| 4.2 | Design and Performance Parameters | 56 |
| 4.3 | Simulating the Approximated Apodization Profiles | 62 |
| 4.4 | Grating Spectrum Calculation..... | 74 |
| 4.5 | Performance Parameters Calculations | 75 |
| 4.6 | Conclusion | 89 |
| 5 | RESULTS AND DISCUSSION | 94 |
| 5.1 | Approximated Gaussian Apodized FBGs..... | 94 |
| 5.1.1 | Performance Parameters Resulted at Fixed Step Size | 97 |
| 5.1.2 | Performance Parameters Resulted at Fixed Maximum Error | 104 |
| 5.2 | Approximated Cosine Apodized FBGs | 107 |
| 5.2.1 | Performance Parameters Resulted at Fixed Step Size | 108 |
| 5.2.2 | Results at Fixed Maximum Error Value | 112 |
| 5.3 | Comparison Between the Gaussian and Cosine Segmented Apodized Gratings..... | 115 |
| 5.4 | Summary and Major Contribution | 121 |
| 6 | CONCLUSIONS..... | 124 |
| | REFERENCES | 128 |
| | APPENDICES | 132 |
| | BIODATA OF THE AUTHOR..... | 158 |

LIST OF TABLES

| TABLE | Page |
|--|-------------|
| Table 1.1: Differences between single and two photon FBG fabrication techniques..... | 5 |
| Table 4.1: Common study parameters | 57 |

LIST OF FIGURES

| FIGURE | Page |
|---|------|
| Figure 2.1: Basic operational principle of FBG [32]. | 16 |
| Figure 2.2: Constructive reflection of the Bragg wavelength. | 17 |
| Figure 2.3: Measured (dots) and calculated (line) reflection spectra for Bragg reflection in a 1mm long uniform grating with $\kappa L = 1.64$ [26]. | 19 |
| Figure 2.4: Schematic diagram for blazed fiber Bragg grating | 21 |
| Figure 2.5: Schematic diagram for chirped fiber Bragg grating | 22 |
| Figure 2.6: Calculated group delay (dashed line) and dispersion (solid line) of a Raised cosine grating with “ac” index change of 5×10^{-4} , zero “dc” index change, FWHM = 10 nm, and a chirp of -1 nm/cm. The inset shows the reflectivity spectrum [26]. | 23 |
| Figure 2.7: Two-beam interferometer arrangement for FBG side writing [11]. | 25 |
| Figure 2.8: Lloyd Interferometer [30]. | 27 |
| Figure 2.9: Prism interferometer [30]. | 27 |
| Figure 2.10: Writing FBG with phase mask technique [12]. | 29 |
| Figure 2.11: Schematic diagram for Talbot interferometer [33]. | 30 |
| Figure 2.12: Schematic diagram for point-by-point fabrication technique [10]. | 31 |
| Figure 2.13: Reflection spectral response for uniform FBGs with $\kappa L = 2$ and $\kappa L = 8$ [26] | 38 |
| Figure 2.14: Calculated reflection spectra (dotted line) and group delay (solid line) for uniform Bragg gratings with $\kappa L = 2$ [26]. | 40 |
| Figure 3.1: Calculated reflectivity spectrum for (a) Tanh (b) Gaussian (c) Raised cosine apodized gratings by IFO_Gratings. | 45 |
| Figure 3.2: Calculated delay spectrum by IFO_Gratings for (a) Tanh (b) Gaussian (c) Raised cosine apodized and chirped gratings. | 47 |
| Figure 3.3: Schematic diagram for interfering beams [33]. | 49 |
| Figure 3.4: Preconditioning UV intensity shaped by the amplitude mask (dashed line) and the fringe profile (solid line) [29]. | 50 |
| Figure 4.1: The error E_{\max} of the segmented apodization profile. | 58 |
| Figure 4.2: Performance parameters calculated by the IFO_Gratings for a 10mm grating with modulation index $= 3 \times 10^{-4}$ apodized with Gaussian profile. | 59 |
| Figure 4.3: Three DWDM channels represented by reflection spectrum of three different gratings to show the crosstalk parameters [35]. | 62 |
| Figure 4.4: Flow chart for the MathCAD program constructed to calculate the approximated apodization profile at fixed step size. | 68 |
| Figure 4.5: The simulated error function along the grating for an approximated profile of maximum error $E_{\max} = 0.02$. | 69 |
| Figure 4.6: Flow chart for the MathCAD program constructed to calculate the approximated apodization profile at fixed value of maximum error. | 73 |
| Figure 4.7: Flow chart for the MathCAD program constructed to calculate the performance parameters for the normal gratings. | 79 |

| | |
|---|-----|
| Figure 4.8: Flow chart for the MathCAD program constructed to calculate the performance parameters for the DWDM gratings. | 83 |
| Figure 4.9: Flow chart for the MathCAD program constructed to calculate the crosstalk parameters for the DWDM gratings. | 88 |
| Figure 4.10: Two segments apodization profile for the Raised cosine function. | 89 |
| Figure 4.11: Approximated apodization profile with step size of $200\ \mu\text{m}$ | 90 |
| Figure 4.12: The spectrum of DWDM grating apodized with an approximated apodization profile with step size of $200\ \mu\text{m}$ | 91 |
| Figure 4.13: Flow chart summarizes the workflow. | 92 |
| Figure 5.1: The number of segments for the approximated Gaussian profile and the maximum error relation. | 95 |
| Figure 5.2: The error function at maximum error of 0.015 for the Gaussian approximated profile after the combination of two segments at the position of 1.7 mm to 3.5 mm. | 96 |
| Figure 5.3: The maximum reflectivity behavior of the approximated Gaussian apodized normal FBGs with varying the maximum error..... | 97 |
| Figure 5.4: The integration of the error function and maximum reflectivity follow the same behavior against the maximum error for the approximated Gaussian apodized FBGs. | 98 |
| Figure 5.5: The approximated Gaussian apodized FBGs Side lobe Suppression ratio and the Integration of error function as a function of maximum error..... | 99 |
| Figure 5.6: Reflectivity spectra for segmented Gaussian apodized normal FBGs with maximum error of 0.014 (solid line) and 0.08 (dashed line). | 100 |
| Figure 5.7: The approximated Gaussian apodized FBGs FWHM bandwidth and the integration of error as a function of maximum error. | 101 |
| Figure 5.8: The Insertion loss of approximated Gaussian apodized DWDM gratings and Integration of error as a function of maximum error. | 102 |
| Figure 5.9: SLSR of the approximated Gaussian apodized DWDM gratings and the integration of the error as a function of maximum error. | 103 |
| Figure 5.10: Adjacent and non-adjacent crosstalk as a function of maximum error for approximated Gaussian apodized DWDM gratings. | 103 |
| Figure 5.11: The bandwidth at -3dB and -20dB for DWDM FBGs apodized with approximated Gaussian profile as a function of maximum error. | 104 |
| Figure 5.12: The maximum reflectivity for normal gratings and insertion loss for DWDM gratings apodized with approximated Gaussian apodization profiles as a function of step size..... | 105 |
| Figure 5.13: SLSR as a function of step size for normal and DWDM approximated Gaussian apodized gratings..... | 106 |
| Figure 5.14: The FWHM bandwidth as a function of step size for the normal and DWDM Gaussian apodized gratings..... | 106 |
| Figure 5.15: The adjacent and non-adjacent crosstalk parameters as function of step size for Gaussian apodized gratings..... | 107 |
| Figure 5.16: The number of segments of the approximated Cosine apodization profiles as function of the maximum error. | 108 |
| Figure 5.17: The maximum reflectivity and the integration of the error as a function of maximum error for approximated Cosine apodized FBGs. | 109 |

| | |
|--|-----|
| Figure 5.18: The SLSR and integration of error for the approximated Cosine apodized FBGs as a function of error..... | 109 |
| Figure 5.19: The FWHM bandwidth for the approximated Cosine apodized FBGs and integration of error as a function of maximum error. | 110 |
| Figure 5.20: The Insertion loss of the approximated Cosine apodized DWDM FBGs. . | 111 |
| Figure 5.21: The segmented Cosine apodized FBGs SLSR for the DWDM grating as a function of error. | 111 |
| Figure 5.22: The crosstalk parameters for approximated Cosine apodized DWDM FBGs. | 112 |
| Figure 5.23: The maximum reflectivity and the insertion loss for normal and DWDM approximated Cosine apodized FBGs as a function of step size. | 113 |
| Figure 5.24: The SLSR of the approximated Cosine apodized normal and DWDM FBGs as function of step size. | 113 |
| Figure 5.25: The segmented Cosine apodized FBGs 3 dB bandwidth as function of step size for (a) normal and (b) DWDM gratings. | 114 |
| Figure 5.26: The adjacent and non-adjacent crosstalk parameters for the segmented Cosine apodized DWDM gratings. | 115 |
| Figure 5.27: The integration of the spatial error as function of maximum error for the Cosine and Gaussian approximated apodization profiles. | 116 |
| Figure 5.28: Number of segments as function of maximum error for Cosine and Gaussian profiles. | 116 |
| Figure 5.29: (a) The maximum reflectivity and (b) The insertion loss for both Cosine and Gaussian gratings with approximated apodization profiles as function of maximum error. | 118 |
| Figure 5.30: The SLSR as function of maximum error for both Cosine and Gaussian gratings with approximated apodization profiles as function of maximum error... | 119 |
| Figure 5.31: FWHM bandwidth as function of maximum error for both Cosine and Gaussian gratings with approximated apodization profiles as function of maximum error (a) normal gratings (b) DWDM gratings. | 120 |
| Figure 5.32: (a) Adjacent and (b) Non-adjacent crosstalk parameters as function of maximum error for both Cosine and Gaussian gratings with approximated apodization profiles..... | 121 |

LIST OF ABBREVIATIONS

| | |
|------------|--|
| AXT | Adjacent crosstalk |
| CRC | Communication Research Center |
| CW | Continuous Wave |
| DFB | Distributed Feedback Grating |
| DWDM | Dense Wavelength Division Multiplexing |
| EDFA | Erbium Doped Fiber Amplifier |
| EMI | Electromagnetic Interference |
| FBG | Fiber Bragg Grating |
| FBGs | Fiber Bragg Gratings |
| FWHM | Full Wave Half Maximum |
| IL | Insertion Loss |
| ITU | International Telecommunication Union |
| MPF | Multiple Printing of in-Fiber Grating |
| NAXT | None Adjacent crosstalk |
| OEC | Optical to Electrical Conversion |
| R_{\max} | Maximum Reflectivity |
| SL | Side lobe |
| SLSR | Side lobe Suppression Ratio |
| SMF | Single Mode Fiber |
| SNR | Signal to Noise Ratio |
| UV | Ultra Violet |
| WDM | Wavelength Division Multiplexing |



CHAPTER ONE

INTRODUCTION

The usage of optical fiber has revolutionized the telecommunication sector. It can transfer the information over very long distances because of its distinguished properties such as the small attenuations at certain wavelengths. Nowadays most of the telecommunication companies are using fiber links, and the fiber market is still increasing. It is believed to be the best media for transferring data in the future.

Wide transmission bandwidth is needed to cover the large demand for telecommunication and the increasing number of data services offered. Most of the services offered are data type services, like the Internet. Thus, the transmission volume of data type information is increasing faster than that of the voice. However, both of them need a high bandwidth transmission media. Optical fiber covers this gap with Wavelength Division Multiplexing (WDM) or Dense WDM (DWDM) transmission techniques. With these methods, four to eight channels (WDM) or more (DWDM) are sent on the same Single Mode Fiber (SMF) that has already been installed. This technique increases the optical fiber importance in telecommunication because it can provide us with a large bandwidth at competitive cost compared to that of other transmission media such as the copper cables, radio links, satellite links, or any other

medium. Moreover, fiber has more advantages such as electromagnetic immunity, high temperature withstanding, lightness, lower costs for long distances, and more security [3,31]. DWDM systems are now being commercially deployed for point-to-point communication links. Recent studies are concentrating to make the DWDM systems work in a network environment.

The discovery of optical fiber photosensitivity opens the way to the DWDM system to become viable. The technology of photosensitive fiber is based on an in-fiber optical filter called Fiber Bragg Grating (FBG). From this basic component, a large number of devices are now available and providing the DWDM system with the basic functions like the multiplexing and channel selection.

1.1 Historical Prospective of FBG

The technological advances related to fiber photosensitivity is relatively recent, and the number of optical devices that depend on these advances in the market is increasing. Wavelength division multiplexers, add/drop multiplexers, and other devices are now available in the market. This makes the DWDM network system easier to be achieved. And they will finally provide with other devices the routing for the DWDM system at the end of the way.

The optical fiber photosensitivity was discovered in 1978 by Hill and Kawasaki [8,14] at the Communication Research Center (CRC) in Canada. They were doing an experiment to study the non-linearity of a specially designed fiber heavily doped with germanium. In this experiment they launched into the core of the fiber a 488 nm intense visible light. And the transmitted and reflected light was measured during the exposure

time. They found out that the transmitted light was attenuated. During exposure, the reflected light intensity was increasing significantly with time. After a specific time all the incident light was totally reflected. The spectral measurements confirmed that this reflection was occurring because of the photo-induced change in the refractive index of the fiber core. This experiment makes an important phenomenon called photosensitivity to be observed for this type of fiber. The increasing interest of researchers in the photosensitivity of optical fiber from then on, led to the production of many photosensitive devices.

The launched light at one terminal of the fiber core interfered with the Fresnel reflected beam from the other terminal of the fiber, to produce a standing wave intensity beam. This standing beam altered the refractive index of the core in this photosensitive fiber at the high intensity points permanently. Thus, the refractive index takes the shape of the intensity of the standing beam, which is a periodic change with the length of the fiber. This refractive index perturbation couple the forward and backward propagating light beams. The reflected beam enhanced the strength of the back-reflected beam, which increases the intensity of the interference pattern. This process continues until the refractive index of the core reaches saturation level.

These first experiments achieved a 90% permanent reflectivity of the incident beam. And the change in the modulated index (Δn) was approximated to be around (10^{-5}) to (10^{-6}) . The bandwidth was measured, by stretching and temperature tuning, to be 200 MHz [11]. The characteristics of this grating were very useful in communication, but the major limitation is that its function is only valid at the visible part of the spectrum around the writing wavelength.

Since then, researchers started to be very interested in the photosensitivity of that special type of fiber presented by Bell Northern Research center which has a small diameter and is heavily doped with germanium. Lam and Garside [16] showed that the magnitude of the refractive index change; depend on the square of the writing power at the argon ion wavelength. This is called the two-photon process. The international interest was not that much at that time because they believed that this property is present only in this special design of fiber. In 1987 Stone [25] proved that the photosensitivity is not a characteristic of only that type of fiber when he demonstrated the same effect on the GeO_2 -doped silica fiber. This ensures that the photosensitivity is a property of many types of fiber. This has ignited worldwide interest in making useful optical fiber devices such as selective spectral filters, DWDM multiplexers, add/drop multiplexers, and other optical devices.

In 1989, Meltz et al. [21] demonstrated the side writing technique. This phenomenon proved to be practical in telecommunication systems. This was done at the United Technology Research Center, and his writing method is called the holographic technique. He found out that the refractive index of the germanium doped fiber core is strongly affected by the side exposure to the single-photon, UV light with a power of 5 eV . Exposing the side of the fiber to interfering beams with 244 nm will produce a modulation in the refractive index of the core. By changing the angle between the interfering beams, the period of interference will be changed accordingly. This makes the reflected beam from this grating to be possible at the (1300-1500 nm) range of wavelength. Even though the phenomenon is still related to the absorption of light in the

Ultra Violet (UV) range, gratings can be fabricated to any wavelength, which makes the grating more practical in the telecommunication and sensing fields.

Afterward, Meltz method was developed to get a modulation index up to (2×10^{-3}) [11]. Further research make it possible to achieve modulation index same as the difference between the refractive index of the core and the cladding. One of the important advantages of the single-photon over the two-photon process is the power needed for each one, to get the same value of modulation index. The two-photon process needs around $1GJ/cm^2$ of influence level for the modulation index to saturate. While the single photon process takes only $1KJ/cm^2$ for the same index change, which is one million times less. Table 1.1 shows some of the major differences between the two methods mentioned above [8,9].

Table 1.1: Differences between single and two photon FBG fabrication techniques

| Property | Two photon process | Single photon process |
|-----------------------|------------------------------------|--|
| Exposure | Internally | Externally |
| Grating length | Along the length of he fiber | Same as the interference length |
| Reflection wavelength | 240-250 nm | 240-1600 nm |
| Influence level | $\approx (1GJ/cm^2)$ to saturate | $\approx (1KJ/cm^2)$ to saturate |
| Popularity | Not used for commercial production | Used for fabrication in industry for mass production |

The most important parameters that affect the modulation index is shown to be the writing beam wavelength, intensity, the exposure time, the composition of the fiber under exposure, and any other pre-processing that may be done to the fiber, like hydrogenation. The laser sources used in fabrication of the Fiber Bragg Gratings (FBGs) are *KrF* and *ArF* excimer lasers, which are UV laser sources operating at 248, and 193 respectively. These lasers generate pulses of laser light each with 1020 ns duration at a frequency of 10's of Hz. A typical example shows that exposing the germanium doped

single mode fiber to a UV laser for several minutes with irradiation intensity of $100 - 500 \text{ mJ/cm}^2$, will produce a refractive index change of magnitude $\Delta n = 10^{-5} - 10^{-4}$ [30,9].

Lamaire et al. [17] showed that optical fiber hydrogenation photosensitize even the standard telecommunication fiber. Loading the fiber with hydrogen before fabrication, produce a very sensitive fiber to the UV light. So gratings with hundred time's higher modulation index were achieved ($\Delta n = 10^{-2}$). This makes the grating a basic component in many linear and non-linear optical devices.

Phase mask was proposed by Hill et al. [12] in 1993 to be used for the fabrication of fiber Bragg gratings (FBGs). The phase mask is a surface relief grating etched in silica plate of glass. It diffracts the UV light beam into several orders, (0, +1, -1, +2, -2....) Depending on its period, the angle of the orders can be controlled, and the efficiency of these orders depends on the mark-space ratio and the etch depth. Special phase masks that have high diffraction efficiency for the plus and minus first orders, and minimum efficiency for the rest of the orders, are used in the fabrication. Exposing this phase mask to the designed UV wavelength will split the beam into the plus and minus orders, which will interfere, just near the opposite side of the phase mask. Placing the fiber a distance close to the diameter of the fiber to the phase mask, will produce a Bragg grating with a period similar to that of the interference pattern which is half the grating pitch period of the phase mask. This technique does not add any improvement on the magnitude of the modulation index, but it relaxes both the high sensitive issue of alignment process needed for the holographic technique, and the stability and quality conditions needed for the laser

source. So it has become the most popular technique especially for the mass production of the fiber gratings.

1.2 Fiber Bragg Grating Applications in Telecommunications

The increasing demand for network bandwidth is principally due to the growth of the data traffic. WDM and DWDM are transmission techniques that provide the networks with the needed bandwidth and speed. These techniques multiplex the data into different wavelength channels, with a constant spacing between them. Using the DWDM systems as a network solution requires many functions to be done in the optical domain, because the Optical to Electrical Conversion (OEC) incurs losses and is a costly option. Devices that provide some of the network functions as DWDM Multiplexers, add/drop Multiplexers and the cross connect may be realized by fiber Bragg gratings [16].

Fiber Bragg gratings are basic components used in many devices because they are in-fiber components and they have unique filtering characteristics. They are used in wavelength-stabilized lasers, fiber lasers, remote pump amplifiers, Raman amplifiers, phase conjugators, wavelength converters, wavelength division multiplexers, add/drop multiplexers, dispersion compensators, and gain equalizers [5,28].

Although the fiber Bragg grating is a band-stop and not a band pass filter, there are solutions to get the desired spectrum in the reflection or transmission of the gratings. Additional devices are required to achieve the desired functionality in the reflection spectrum, such as circulators and couplers. On the other hand, solutions like distributed feedback (DFB) gratings, Fabry-port interferometer, moiré resonator, and slide tap filters